Journal of Polymer Science and Engineering 2026, 9(2), 026200010.
https://doi.org/10.24294/jpse026200010

Article

Morphological and correlation characteristics of polymer-liquid crystal systems

Mukhtor Egamov[1,2,*], Ma'ruf Yorov[1], Umeda Rakhimova[1]

[1] Khujand Scientific Center of the National Academy of Sciences of Tajikistan, Khujand 735714, Tajikistan
[2] Mining and Metallurgical Institute of Tajikistan, Buston 735730, Tajikistan
*** Corresponding author:** Mukhtor Egamov, egamov62@mail.ru

CITATION

Egamov M, Yorov M, Rakhimova U. Morphological and correlation characteristics of polymer-liquid crystal systems. Journal of Polymer Science and Engineering. 2026; 9(2): 026200010. https://doi.org/10.24294/jpse026200010

ARTICLE INFO

Received: 14 May 2026
Accepted: 13 July 2026
Available online: 24 August 2026

Abstract: A method for producing polymer-encapsulated liquid crystal (PELC) films based on polyvinyl butyral (PVB) as a binder and 4-n-pentyl-4'-cyanobiphenyl (5CB) as a liquid crystal (LC) has been proposed, along with an analysis of their optical characteristics. The PELC films were obtained by the phase separation during heating (TIPS) method with different compositions of the two components. Detailed studies were conducted using polarized optical microscopy (POM) and derivatography to assess the correlation between the composition of the composite and the formation of PELC. It was found that PVB and 4-n-pentyl-4'-cyanobiphenyl (5CB) are partially miscible, with the maximum solubility limit lying in the range (41–43%). The presented thermograms and their analysis expand the current understanding of the formation of PELCs using the TIPS method. The use of PVB as a binder in the creation of CPLC systems opens up new design possibilities due to its superior performance compared to other polymers commonly used in composite systems. PVB has been proven to be an ideal binder material for the formation of PELC films.

Keywords: encapsulation; polyvinyl butyral; liquid crystal; morphology; phase transition; texture; mesophase; droplet; nematic

1. Introduction

The synthesis of functional materials is routinely accomplished through well-understood processes involving the melting and intermixing of monomeric and polymeric precursors. Contemporary research has increasingly focused on mesomorphic precursors, exemplified by liquid crystals. A principal practical application stemming from these investigations is the development of polymer-encapsulated liquid crystal (PELC) films, which are manufactured via polymerization-induced phase separation (PIPS). PELC constitute a novel class of materials that are highly promising for applications in switchable (smart) windows and projection display technologies [1–4]. The potential implementation of PELC films as optical information storage media [5] or as capacitors in reliable microscale energy-harvesting systems [6] further enhances the attractiveness of these materials. In a typical PELC system, liquid crystal (LC) droplets, measuring around 3 to 25 μm (μm), are encapsulated throughout a solid polymer. These tiny droplets are the key to the material's distinctive capabilities. Applying an external electric field allows us to manipulate the orientation of the LC molecules, thereby enabling effective regulation of transmitted light intensity. A key advantage of PELC materials is the relative simplicity of their fabrication process. They have been fabricated using various techniques, including encapsulation (emulsification) and phase separation, with the latter becoming the predominant production method [7–9]. Creating PELC materials

is most straightforward when a liquid crystal and a thermoplastic polymer are first blended into a uniform liquid state and then cooled. The effectiveness of PELC systems is significantly shaped by the way the liquid crystal droplets are arranged within the polymer. The size, shape, and spatial distribution of the LC domains are governed not only by thermodynamic phase equilibrium but also depend critically on the types of polymers and liquid crystals employed, as well as on interfacial interactions [7,8]. Research indicates that the electro-optical characteristics of PELC systems are highly sensitive to the selection of their constituent materials. The polymer, being a crucial element within PELCs, plays a significant role in determining their electro-optical behavior. Various polymer matrices have been employed in PELC systems, including polystyrene (PS), polymethyl methacrylate (PMMA), polyacrylate (PA), polyvinyl alcohol (PVA), and the UV-curable resin NOA65 (Norland Products, Cranbury, New Jersey, USA) [10–13].

Among the polymers listed above, another thermoplastic material—polyvinyl butyral (PVB)—has attracted attention, as its use as a component in composite formulations may play a significant role in the development of high-performance materials with tailored properties [14,15]. However, there is limited scientific literature regarding PVB as a binding material for composite systems. In this investigation, we examine the process of forming PELC films, with PVB acting as the polymer backbone. The article presents the preparation and thermotropic characteristics of a liquid crystal composite built from the nematic liquid crystal 5CB and polyvinyl butyral (PVB). The PELC samples were manufactured using the TIPS approach, with varying proportions of the two components. A thorough examination utilizing POM and DSC was performed to establish the relationship between the composite's composition and the morphology of the produced films. The principal objective of this research is the development of PELC systems that employ PVB as the polymer matrix, due to its superior performance as a structural material. A systematic mechanism has been devised for the creation of stable PELC films appropriate for optical applications.

2. Experiment

2.1. Polymer matrix

Polyvinyl butyral (PVB) purchased from Merck was chosen as the binder. This polymer belongs to the family of high-performance thermoplastics obtained by reacting the acetylation product of polyvinyl alcohol with butyraldehyde. The backbone of the polymer chain is derived from the polyvinyl alcohol chain, but without hydroxyl substituents: during the polymer-analogous transformation, hydroxyl groups react with protonated butyraldehyde molecules; as a result, a fundamentally new structure is being formed. PVB is a semi-rigid linear-chain polymer distinguished by its superior mechanical strength, elevated service temperature relative to other melt-processable thermoplastics, minimal creep deformation, favorable dielectric characteristics, optical transparency, and pronounced resistance to lubricants, numerous solvents, and a wide range of chemical agents. Its enhanced thermal stability renders PVB particularly suitable for advanced electronic applications, especially under conditions involving exposure to vapor-phase

environments or infrared soldering temperatures. Notably, the material preserves its functional and structural properties within the temperature interval of 100–150 ℃. Furthermore, PVB demonstrates remarkable chemical resistance toward mineral acids, alkaline media, and electrolyte solutions over a broad pH range extending from 2 to 13. PVB exhibits substantial resistance to oxidizing agents, thereby permitting cleaning procedures involving bleaching compounds. In addition, the polymer demonstrates notable stability in the presence of surfactants and hydrocarbon-based oils. Furthermore, PVB exhibits good chemical resistance toward mineral acids, alkaline media, and electrolyte solutions over a broad pH range (2–13), as well as stability in the presence of surfactants and hydrocarbon-based oils. It is, however, readily soluble in polar solvents such as short-chain alcohols, a property exploited in the present study, where PVB was dissolved in ethanol to prepare the composite solutions. PVB is also soluble in or swollen by ketones, esters, and chlorinated or aromatic hydrocarbons, which limits its use in applications requiring resistance to these solvent classes. From a mechanical standpoint, PVB is characterized by high compressive strength, which enables its effective utilization in applications subjected to elevated pressure conditions. Due to its relatively low raw material and processing costs, PVB is employed in specialized applications and often serves as an excellent alternative to polycarbonates. PVB facilitates the straightforward fabrication of membranes suitable for a broad range of applications, including wastewater treatment, food and beverage processing, and gas separation technologies. In the present study, a transparent grade of PVB was utilized, exhibiting a glass transition temperature of 58 ℃, as determined by differential scanning calorimetry (DSC) during the initial heating cycle (1 h) conducted at a heating rate of 20 ℃ min^{-1}.

2.2. Liquid crystal

As the nematic component, a single-component liquid crystal of the 4-n-pentyl-4′-cyanobiphenyl type (5CB) [16] was employed. This choice of CN-terminated liquid crystal was motivated by the chemical stability of CN-containing LCs, their short relaxation times, and high optical anisotropy. Such materials are extensively employed in liquid crystal display (LCD) technologies. The prepared mixtures were subsequently dried in a thermal oven at 50 ℃ for 24 h. The molecular structure of the nematic liquid crystal (NLC) compound 5CB was verified using DSC and elemental analysis techniques.

The physicochemical properties of the nematic liquid crystal 5CB were further characterized and confirmed by means of polarized optical microscopy (POM) and differential scanning calorimetry (DSC).

2.3. Preparation of CPLC Films

Polymer-encapsulated liquid crystal (PELC) composites were fabricated employing thermally induced phase separation (TIPS) and solvent-induced phase separation (SIPS) methodologies. NLC 5CB and PVB were combined in various weight ratios (**Table 1**) and subsequently dissolved in ethanol (C_2H_5OH) to prepare a 5 wt.% solution.

Table 1. Compositions used for PELC preparation.

Code	P1N9	P2N8	P3N7	P4N6	P5N5	P6N4	P7N3	P8N2	P9N1
PVB	10	20	30	40	50	60	70	80	90
5CB	90	80	70	60	50	40	30	20	10

The prepared solutions were subjected to magnetic stirring for 0.5 h to achieve complete homogenization, after which they were cast onto glass substrates and maintained at room temperature for 24 h. Subsequently, the samples were dried in a constant-temperature oven (BOV-T70C) for an additional 24 h to ensure efficient solvent evaporation and complete removal of residual ethanol.

For the preparation of PELC films using the polymerization-induced phase separation (PIPS) technique, the obtained films were heated to 80 ℃, i.e., above the glass transition temperature (T_g) of PVB, at a heating rate of 20 ℃ min^{-1} to promote uniform mixing of the components. The films were then cooled at a controlled rate of 10 ℃ min^{-1}. In this manner, well-defined PELC films were obtained for the specific mixture compositions, and their formation was monitored using polarized optical microscopy (POM) [11].

2.4. Research methods

Differential scanning calorimetry (DSC) thermograms were obtained during successive heating–cooling cycles, employing a heating rate of 20 ℃ min^{-1} and a cooling rate of 10 ℃ min^{-1} over the temperature range of 20–180 ℃. The measurements were carried out using a Netzsch DSC instrument (DSC BK-DSC 300L) under a nitrogen atmosphere. The glass transition temperature (T_g) was defined as the midpoint of the baseline step change, whereas the temperatures of first-order phase transitions were identified from the corresponding peak maxima.

The phase behavior of NLC 5CB and the PELC composites was further investigated using polarized optical microscopy (POM) with a POLAM-2 microscope equipped with a MYscope 500 M digital video camera (Webbers), enabling both photographic and video recording of the ongoing processes.

3. Results and discussion

Polarized optical microscopy (POM) and differential scanning calorimetry (DSC) were utilized to characterize both the pure constituents and the fabricated PELC films. These techniques enabled the evaluation of the spatial organization and structural distribution of the liquid crystalline phase within the polymer matrix. DSC analysis of neat PVB exhibited a glass transition temperature at 58 ℃ (**Figure 1**).

For NLC 5CB, DSC thermograms have three endotherms during heating and two exotherms during cooling. According to the observations of the POM, the maxima of DSC were distributed as follows: the transition from solid to solid, corresponding to the first endotherm when scanned under heating (51 ℃), the mesophase transition from the crystalline state to the nematic phase for the second endothermic maximum, and isotropization for the last endothermic maximum (**Figure 1**). According to [17], the endothermic the maximum attributed to the transition from the crystalline to the nematic phase has a higher enthalpy compared to the maximum due to the transition

from the nematic phase to the isotropic state (**Table 2**). The reason for the appearance of topological defects is the incompatibility of the boundary conditions between the planar-orienting substrate and the convex surface, where the LC molecules are oriented homotropically. The radially symmetric structure with a point defect indicates a degenerate planar orientation on transparent substrates. Rotating the substrates leads to the removal of the planar orientation degeneracy and a structural transition with a change in the charge of the topological defect. The weak exothermic maximum is attributed to the isotropic-to-nematic phase transition, whereas the more intense exothermic maximum corresponds to the nematic-to-crystalline transition. Upon cooling, the solid–solid transition is no longer observed. The nematic mesophase exhibits a marble-like texture upon heating and a Schlieren texture with two- and four-brush patterns [18] upon cooling (**Figure 2a,b**), remaining stable over a wide temperature range up to 66 ℃.

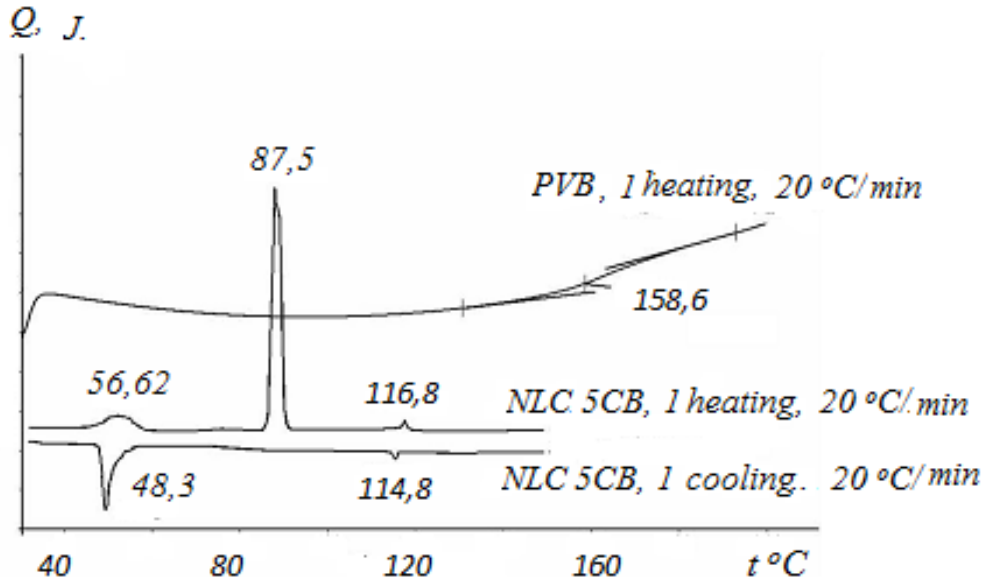

Figure 1. DSC thermograms for NLC (5CB).

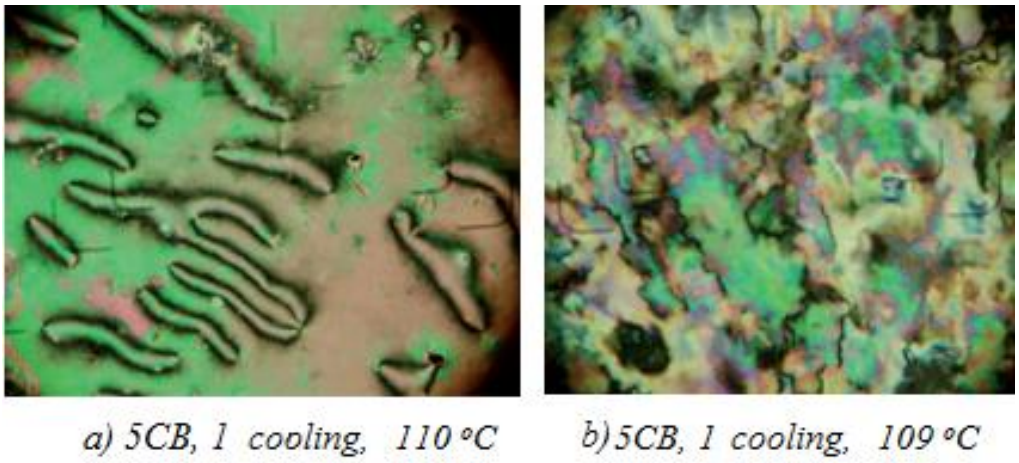

Figure 2. Optical micrographs of 5CB composites recorded at different temperatures using (**a**) polarized optical microscopy and (**b**) crossed polarizers.

Table 2. Summary of the thermotropic phase behavior of PELC films.

Code	T_g (T_m^1)	T_{S-S} (ΔH)	T_m^2 (ΔH)	T_i (ΔH)	T_{Cr} (ΔH)	POM
5CB	-	56.62	87.5	114.78	48.32	Marble and Schlieren texture
P1N9	-	65.87	86.4	108.62	46.92	Thermotropic behavior
P2N8	-	50.75	85	102.58	42.23	Large drops when cooling
P3N7	55.1	-	84.3	-	36.37	Small drops when cooling
P4N6	52	-	86.8	-	42.23	Small drops when cooling
P5N5	62	-	86.4	98.4	39.19	Large drops when cooling
P6N4	63	-	62/7	77.5	-	Fine texture when first heated
P7N3	49.9	-	56.3	-	-	Rarely falling drops during cooling
P8N2	82.7	-	-	-	-	Fine texture when first heated
P9N1	102.38	-	-	-	-	Amorphous phase
PVB	156	-	-	-	-	Amorphous phase

Notes: T_g denotes the glass transition temperature; T_{1m} corresponds to the melting temperature of the polymer matrix enriched with liquid crystals; T_{2m} refers to the melting temperature of the liquid crystal phase; T_i indicates the isotropization temperature; and T_{Cr} represents the crystallization temperature. All temperatures are expressed in °C. ΔH denotes the enthalpy change, reported in J g^{-1}.

Composites with the highest concentrations of NLC 5CB (P1N9 and P2N8) exhibit DSC profiles closely resembling those of the neat (pristine) liquid crystal, with the principal distinctions being marginal decreases in the melting temperatures (by 1 ℃ and 2 ℃, respectively) and in the isotropization temperatures (by 6 ℃ and 12 ℃, respectively). This behavior may be ascribed to the presence of minor amounts of PVB, which acts as a diluent/impurity within the system, thereby slightly perturbing the phase transition temperatures.

A more detailed analysis of the thermograms reveals, in addition, a weak exothermic maximum at approximately 0 ℃. Polarized optical microscopy (POM) observations indicate a marble-like texture for P1N9, closely resembling that of neat 5CB, whereas P2N8 exhibits the formation of large droplets during cooling (**Figure 3a**). On the basis of these findings, the more pronounced exothermic maximum observed at approximately 40 ℃ is attributed to the crystallization of larger droplets, while the weaker exothermic maximum near 0 ℃ is assigned to the crystallization of smaller droplets.

Composites containing intermediate amounts of NLC 5CB (P3N7, P4N6, and P5N5) clearly exhibit phase separation upon cooling, forming small, round droplets with birefringence dispersed within the polymer binder [19] (**Figure 3b–d**). The inherent scheme for the orientational structure with two budjums (black semicircles) and defects in the ring surface (cross-section indicated by squares) is shown in the right part of **Figure 3** under the symbol (d). The bipolar axis is oriented horizontally, as in **Figure 3a**. In the schematic representation, the symbol α represents the angle of inclination between the local orientation of the director and the normal to the surface. In all observed images, the droplet size is 10 μm.

As can be seen, the upper and lower defects are connected by a dark line. At the same time, the boundary of the droplet is clearly visible all around. This indicates that the director is oriented mainly parallel to the polarizer. The vertical thin extinction band connecting the upper and lower defects at the boundary, and the horizontal

extinction band connecting the two other defects, are also visible in the crossed polarizers (**Figure 3a**, top row). Moreover, four extinction regions are close to each other in the droplet and are located. Rotating the sample 45º clockwise relative to the polarizers completely changes the optical texture observed in both crossed polarizers and without the analyzer (**Figure 3c**). In crossed polarizers, an interference color pattern appears in the absence of an extinction band. Four identical regions along the droplet boundary are also visible without the analyzer. As the droplet moves clockwise, maximum darkening occurs in the characteristic regions. Then, the sharpness of the boundary gradually decreases until the next image.

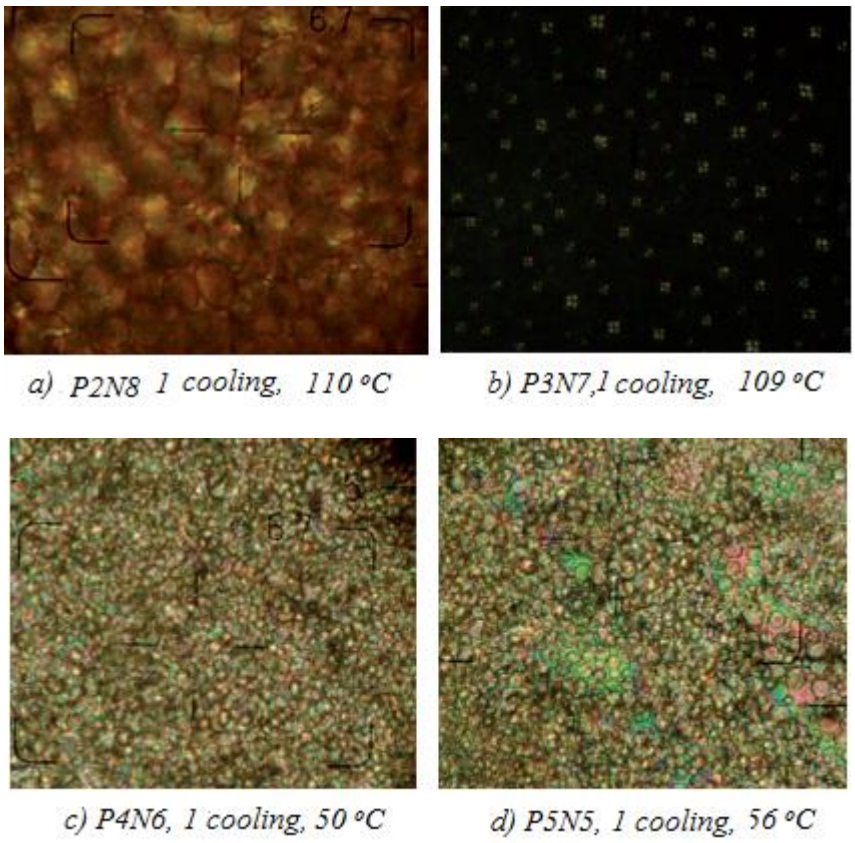

Figure 3. Micrographs of PELC composites at different temperatures obtained by (**a**, **c**) polarized optical microscopy and (**b**, **d**) crossed-polarizer imaging.

The optical structure shown in **Figure 3d** is similar to the pattern obtained without the analyzer (**Figure 3b**). Therefore, when the analyzer is turned off, the boundaries of the droplet lose their clarity. By comparing the extinction band (**Figure 3**, top row) with the preferred orientation of the director at the edge of the droplet (**Figure 3**, bottom row), it is possible to determine the angle of inclination α between the director and the N normal to the surface (**Figure 3d**). The director may be parallel to any horizontal or vertical polarizer in the extinction region located at the bottom left (**Figure 3**, top row). However, observations of the droplet without an analyzer revealed that the director is approximately horizontal.

Phase separation is already evident within the isotropic phase of 5CB under normal illumination (**Figure 4a**). Crystallization of the nematic droplets was not detected by polarized optical microscopy until the samples reached room temperature.

DSC analysis revealed a broad, weak endothermic feature upon heating at approximately 55 ℃ for P3N7, which appears only as a faint shoulder at around 62 ℃ for P5N5, together with a pronounced maximum near 85 ℃ corresponding to the crystalline-to-nematic mesophase transition (**Figure 5**). The endothermic isotropization maximum is observable only for P5N5, whereas for P4N6 it manifests as a very weak and broadened feature, and for P3N7 it is not discernible within the heating scan.

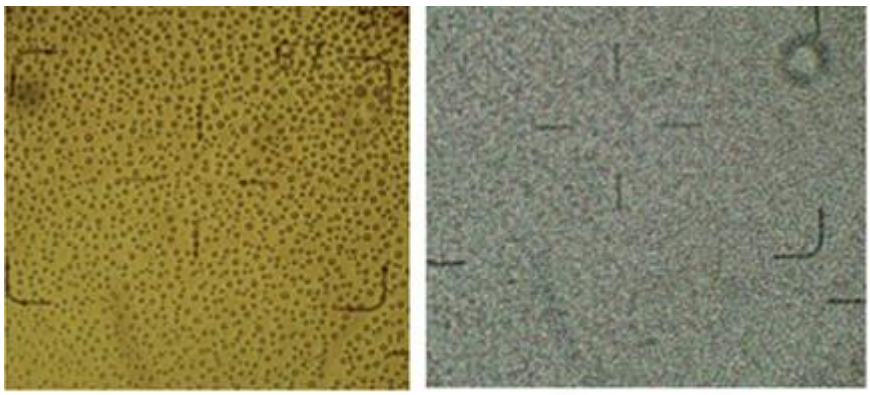

Figure 4. Micrographs of composites P4N6 and P8N2 at 180 ℃ obtained by (**a**) polarized optical microscopy and (**b**) crossed-polarizer imaging.

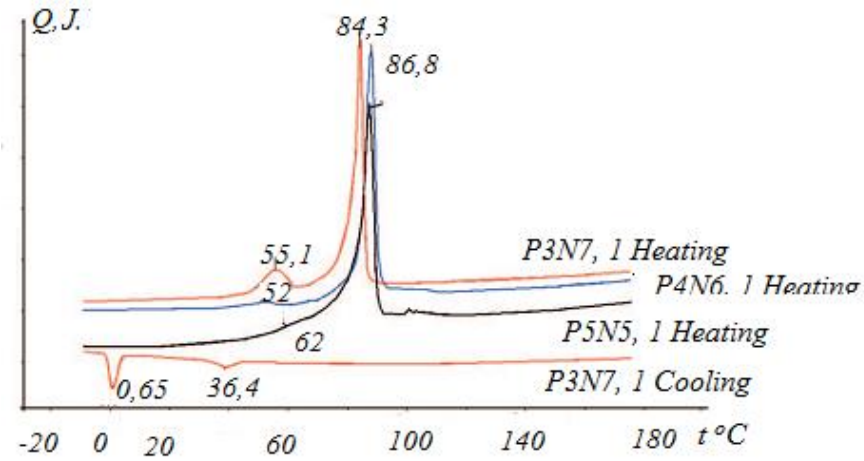

Figure 5. DSC curves of composites containing intermediate fractions of NLC 5CB.

During cooling scanning, the maximum corresponding to the divergence temperature did not appear, probably due to the encapsulation of the liquid crystal in the form of small droplets, whose transitions between enlightenment and divergence occur with a minor difference. It is for this reason that the corresponding enthalpy change could not be measured in DSC, which prevented the analysis of this transition, which is well known to be based on a small enthalpy change [19,20].

Isotropization temperatures were determined from POM observations (**Table 2**). In the cooling curves, two distinct exothermic events are observed: a weak maximum at approximately 40 ℃ and a more pronounced maximum near 0 ℃, indicative of a

two-step crystallization process associated with droplets of different size distributions. By comparison with the thermal behavior of P1N9 and P2N8, the intense exothermic maximum at 0 ℃ is assigned to the crystallization of small droplets, whereas the weaker maximum at 40 ℃ corresponds to the crystallization of larger droplets. The lower crystallization temperature observed for the small droplets suggests a reduced level of polymer contamination within these domains relative to the larger droplets.

By comparing the enthalpy changes associated with both crystallization events, it can be inferred that an increase in polymer content within the composites promotes a higher proportion of small droplets relative to large ones. Moreover, analysis of the total crystallization enthalpy across all samples reveals a progressive decrease with increasing polymer concentration, which is likely attributable to a reduced liquid crystal fraction within the dispersed phase, arising from enhanced dissolution of 5CB in the polymer binder. Under these conditions, the initial endothermic event in the DSC profiles corresponds either to melting (for P3N7 and P4N6) or to the glass transition (for P5N5–P9N1) of the liquid crystalline component dispersed within the polymer binder.

For the P6N4 and P7N3 composites, the DSC thermograms display two broad endothermic maxima upon heating, corresponding to the melting and subsequent isotropization of the homogeneous mixtures (**Figure 6**). In contrast, during the cooling cycle and the second heating scan, only DSC detects the glass transition. However, POM observations during cooling reveal the presence of a limited number of dispersed liquid crystal droplets [21].

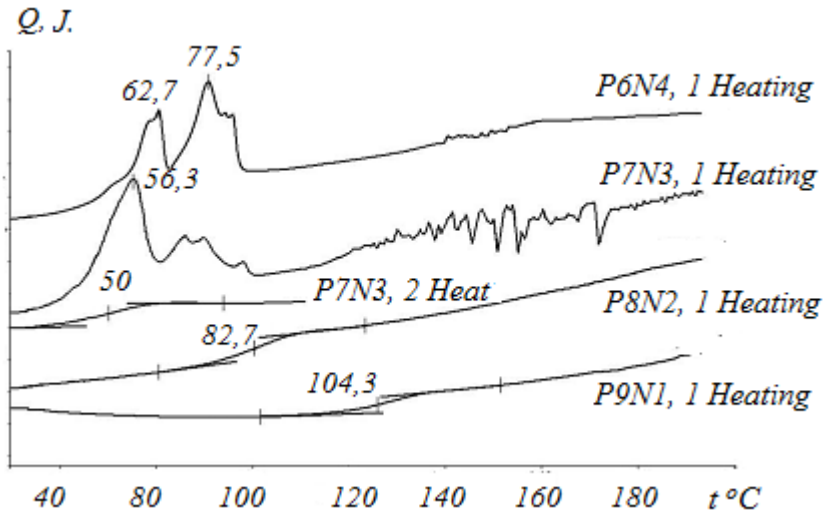

Figure 6. DSC curves of composites containing low fractions of NLC 5CB.

For the P8N2 and P9N1 composites, the DSC thermograms are similar to those of pure PVB. This indicates that the low 5CB content in these composites (10 % and 20 % respectively) is insufficient to induce phase separation; the LC is dissolved in the polymer and acts only as a plasticizer, reducing the glass transition temperature of the polymer binder. In POM films, which are obtained by heating/cooling, are isotropic in polarized light and show fine granulation in normal light (**Figure 4b**). DSC and POM data are given in **Table 2**. The value of the surface tension of a NLC droplet

on an anisotropic surface depends on the direction between the nematic director and the tangent to the droplet contour. This dependence manifests itself in the fact that the contours of droplets deposited on an oriented surface have an elliptical shape, with the diametric disclination predominantly oriented along the minor axis of the ellipse, as the highest cohesive energy corresponds to the oppositely directed dipole moments of 5CB and PVB. Since the droplets are quite large (≅0.85 mm), their ellipticity is very close to 1, but the observation of the modified shape of the droplets on the oriented surface is evident. Let us consider the behavior of an LC drop on a sensitive PVB surface. Based on elementary geometric considerations, the following relations can be written:

$$r_0 \cos\alpha(x) = r_0 - h_0 + h(x)$$

$$\cos\alpha(x) = 1 - \frac{x^2}{2r_0^2}$$

Assuming that $\alpha \le \theta_0$, we can show the parabolic dependence of h(x):

$$h(x) = h_0 - \frac{x^2}{2r_0^2}$$

Since angle $\alpha \cong 8 - 13°$, then $\alpha(x) = \frac{x}{r_0}$ [18]. Then the functional dependence of the solubility limit between PVB and NLC 5CB is as follows:

$$T(x) = \sin^2\left(\frac{\pi}{\lambda}\int_0^{h(x)} \Delta n_{eff}(x,z)\,dz\right)$$

where

$$\Delta n(x,z) = \frac{n_o n_e}{\sqrt{1+\left(n_e^2 - n_0^2\right)\cos^2\alpha(x,z)}} \text{-}n_0$$

effective refractive index. In the absence of external fields, the dependence of the NLC solubility limit of the polymer matrix is linear from 0 to α(x) on the surface of a glass transparent substrate. Therefore, using the extrapolation method, we can determine the maximum solubility limit, which is 42.8% in our case.

By combining DSC and POM data for the initial (pure) components and all the composites studied in this work, we concluded that this process does not lead to complete separation of the two components, and a certain amount of the 5CB NLC fraction remains in the polymer matrix, acting as a plasticizer and reducing the glass transition temperature of the binder.

4. Conclusions

Using the TIPS method, novel PELC systems were prepared with PVB as the polymer binder and the low-molecular-weight NLC 5CB. Microscopic analysis

revealed the formation of well-defined LC droplets upon cooling in composites containing 70%, 60%, and 50% nematic 5CB.

DSC measurements corroborated the POM observations, indicating that PVB and 4-n-pentyl-4′-cyanobiphenyl (5CB) exhibit partial miscibility, with a maximum solubility limit of 42.8%. The reported thermal behavior and corresponding analysis extend the current understanding of CPLC formation via the TIPS method. The application of PVB as a polymer binder in CPLC systems thus offers new prospects for material design, owing to its superior performance characteristics relative to conventional polymers commonly used in such systems.

Acknowledgments: The authors express their gratitude to the Ministry of Finance of the Republic of Tajikistan for the financial support provided under Project 0121TJ1107 dated March 10, 2021.

Conflict of interest: The authors declare no conflict of interest.

References

1. Drzaic PS. Liquid Crystal Dispersions. Singapore: World Scientific Publishing; 1995.
2. Blinov LM, Chigrinov VG. Electrooptic Effects in Liquid Crystal Materials. New York, NY: Springer-Verlag; 1994.
3. Mucha M. Polymer as an important component of blends and composites with liquid crystals. Progress in Polymer Science. 2008; 28(5): 837–873. doi: 10.1016/S0079-6700(02)00120-7
4. Dierking I. Textures of Liquid Crystals. Weinheim, Germany: Wiley-VCH; 2006. doi: 10.1002/3527602796
5. Scholes S, Mohapi L, Leach J, et al. Experimentally simulating the beam shaping capabilities of piston-type deformable mirrors using a liquid crystal spatial light modulator. Applied Physics B. 2023; 129(45): 1–7. doi: 10.1007/s00340-023-07991-3
6. Liu YJ, Ding X, Lin SCS, et al. Surface acoustic wave driven light shutters using polymer-dispersed liquid crystals. Advanced Materials. 2011; 23(14): 1656–1659. doi: 10.1002/adma.201004158
7. Emelyanenko AV, Rudyak VY, Shvetsov SA, et al. Transformation of polar nematic phases in the presence of an electric field. Physical Review E. 2024; 109: 014701. doi: 10.1103/PhysRevE.109.014701
8. Loiko VA, Krakhalev MN, Konkolovich AV, et al. Experimental results and theoretical model to describe angular dependence of light scattering by monolayer of nematic droplets. Journal of Quantitative Spectroscopy and Radiative Transfer. 2016; 178: 152–157. doi: 10.1016/j.jqsrt.2015.12.011
9. Marin L, Ailincai D, Paslaru E. Monodisperse PDLC composites generated by use of polyvinyl alcohol boric acid as matrix. RSC Advances. 2014; 4(72): 38397–38404. doi: 10.1039/C4RA05905K
10. Sokolovskaya OI, Nesterov VY, Presnov ND, et al. Diagnostics of ultraviolet-induced isotropic phase transitions in nematic liquid crystal with azochromophore. Liquid Crystals and their Application. 2025; 25(1): 90–98. (In Russian) doi: 10.18083/L.C.Appl.2025.1.90
11. Shih W, Chung SY, Chen YY, et al. Tunable capacitor based on polymer-dispersed liquid crystal for power harvesting. IEEE Transactions on Electron Devices. 2008; 55(10): 2568–2573. doi: 10.1109/TED.2008.2003023
12. Wang J, Xia J, Hong SW, et al. Phase separation of polymer-dispersed liquid crystals on a chemically patterned substrate. Langmuir. 2007; 23(13): 7411–7415. doi: 10.1021/la070278z
13. Mhatre MM, Katariya-Jain A, Deshmukh RR. Improved electro-optical and dielectric properties of polymer-dispersed liquid crystal doped with disperse dye red 1 and carbon nanoparticles. Liquid Crystals. 2023; 50(6): 957–976. doi: 10.1080/02678292.2023.2185564
14. Chekulaev IS, Simushkina SV, Kovalev YV, et al. Dispersion of the anisotropy of the refractive index of a liquid crystal in a low-temperature nematic phase. Bulletin of the Federal State University of Education, Series: Physics and Mathematics. 2025; (3): 76–89. (In Russian) doi: 10.18384/2949-5067-2025-3-76-89
15. Egamov MK. Studies of the structure and properties of polymer-dispersed liquid crystal films to create a polarizer. Journal of Polymer Science and Engineering. 2024; 7(2): 132–144.

16. Gray GW, Harrison KJ, Nash JA. New family of nematic liquid crystals for displays. Electronics Letters. 1973; 9(6): 130–131. doi: 10.1049/el:19730094
17. Mansare T, Decressain R, Gors C, et al. Phase transformations and dynamics of 4-cyano-4’-pentylbiphenyl (5CB) by nuclear magnetic resonance, differential scanning calorimetry, and wide-angle X-ray diffraction analysis. Molecular Crystals and Liquid Crystals. 2002; 382(1): 97–111. doi: 10.1080/713738808
18. Egamov MK. Rotations of the polarization plane of light radiation in nematic liquid crystals. Fundamental Problems of Modern Materials Science. 2024; 21(2): 199–204.
19. Marin L, Cozan V, Bruma M. Comparative study of new thermotropic polyazomethines. Polymers for Advanced Technologies. 2006; 17(9–10): 654–672. doi: 10.1002/pat.764
20. Lin YH, Cheng WC, Reshetnyak V, et al. Electrically tunable gradient-index lenses via liquid crystals: beyond the power law. Optics Express. 2023; 31(23): 1–18. doi: 10.1364/OE.50458
21. Plewa J. Examples of auxetic structures with phase transition. Academy of Materials Science. 2025; (2): 1–12. doi: 10.20935/AcadMatSci7812